ELSEVIER Nuclear Instruments and Methods in Physics Research A 422 (1999) 562–566

NUCLEAR INSTRUMENTS & METHODS IN PHYSICS RESEARCH Section A

The Lunar Prospector gamma-ray and neutron spectrometers

W.C. Feldman[a,*], B.L. Barraclough[a], K.R. Fuller[a], D.J. Lawrence[a], S. Maurice[a], M.C. Miller[a], T.H. Prettyman[a], A.B. Binder[b]

[a] *Los Alamos National Laboratory, MS-D466, Los Alamos, NM 87545, USA*
[b] *Lunar Research Institute, Gilroy, CA 95020, USA*

Abstract

Gamma-ray and neutron spectrometers (GRS and NS, respectively) are included in the payload complement of Lunar Prospector (LP) that is currently orbiting the Moon. Specific objectives of the GRS are to map abundances of O, Si, Fe, Ti, U, Th, K, and perhaps, Mg, Al, and Ca, to depths of about 20 cm. Those of the NS are to search for water ice to depths of about 50 cm near the lunar poles and to map regolith maturity. The designs of both spectrometers are described and their performance in both the laboratory and in lunar orbit are presented.

1. Introduction

Lunar Prospector carries a gamma-ray spectrometer (GRS) and a neutron spectrometer (NS) which together, will provide global maps of the major element (O, Si, Fe, Ti, and perhaps Mg, Al, and Ca) and trace element (U, Th, K, and H) composition of the lunar surface. Special emphasis is placed on the search for polar water-ice deposits as implied by the H abundances. The gamma-ray detector is mounted on one of three 2.5 m science booms and the neutron detector is mounted on a second boom. The spacecraft is spin stabilized about an axis that is nearly perpendicular to the ecliptic plane.

* Corresponding author. Tel.: +1 505 667 7372; fax: +1 505 665 7395; e-mail: wfeldman@lanl.gov.

2. The gamma-ray spectrometer (GRS)

The gamma-ray spectrometer (GRS) consists of a 7.1 cm diameter by 7.6 cm long cylinder of bismuth germanate (BGO) placed within a well-shaped borated-plastic scintillator (BC454) anti-coincidence shield (ACS), as shown in Fig. 1. The ACS is 12 cm diameter, 20 cm long and contains a 10 cm deep by 8.4 cm diameter cylindrical cutout on one end that houses the BGO crystal.

The GRS front-end electronics is configured to classify each detected event into one of four categories: (1) an isolated BGO interaction, (2) a single coincident BGO and ACS interaction, (3) a time-correlated pair of ACS interactions that occur within 25.6 μs, and (4) a time-correlated pair of ACS interactions where the second of the pair consists of a coincident BGO and ACS interaction. Continuous gain calibration is obtained using the

0168-9002/99/$ – see front matter
PII: S0168-9002(98)00934-6

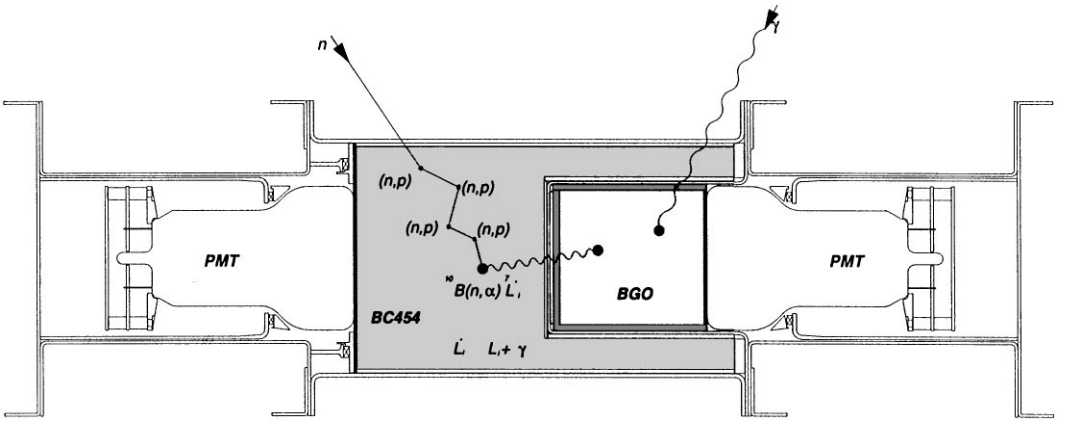

Fig. 1. A simplified drawing of the Lunar Prospector gamma-ray spectrometer. Examples of all four categories of interactions are illustrated at the top. A gamma ray that interacts in the BGO without interacting in the anticoincidence shield (ACS, shown at the upper right) is a category 1 event. An incident neutron (shown at the upper left) that deposits all of its energy by way of multiple (n,p) scattering in the ACS yields either a single (Category-2) or double (Category-3 or -4) pulse depending on its energy.

$^{10}B(n,\alpha)^{7}Li^{*}$ reaction in the ACS in coincidence with a 478 keV gamma ray from deexcitation of $^{7}Li^{*}$ to its ground state, which is detected by the BGO.

The thermal shield of the GRS was designed to allow operation of the BGO at a temperature of about $-28^{\circ}C$ in order to make use of the fact that the light output of BGO for a given energy input increases with decreasing temperature [2]. Measurement of the gain in light output of the flight GRS BGO using a ^{137}Cs source yields a factor of 1.5 increase when its temperature is decreased from 22°C to $-28^{\circ}C$. This gain, in turn, reduces the full-width at half maximum (FWHM) energy resolution at 0.662 MeV from about 12.5% at 22°C to 10.5% at $-28^{\circ}C$. The percent FWHM scales as $E^{-0.5}$.

512-channel gamma-ray spectra, both accepted (Category 1 events) and rejected (Category 2 events) by the ACS, are recorded separately and telemetered to Earth. This feature allows for a considerable reduction in the Compton continuum and 0.511 MeV escape peaks of gamma-ray line shapes by subtracting a multiple of the rejected spectrum from the accepted spectrum after receipt on the ground. A demonstration of this capability is given in Fig. 2 using a thin ^{137}Cs isotopic source. The

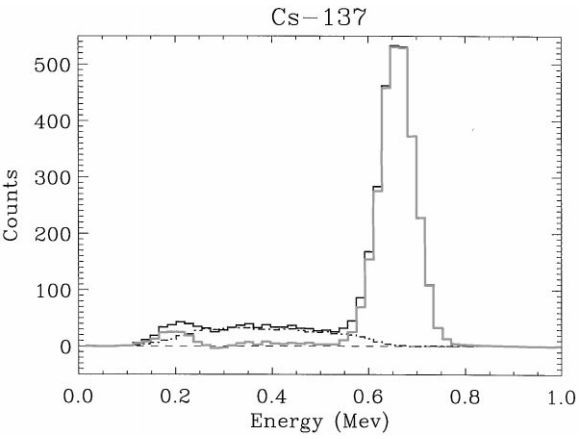

Fig. 2. Pulse height spectra of accepted (A), rejected (R), and ($A - 1.3R$) measured by the GRS using a thin ^{137}Cs source that illustrate its ability to remove the Compton continuum.

source was positioned 1 m from the GRS and oriented perpendicular to the symmetry axis of the detector. Room background was subtracted from all spectra. The three traces in each spectrum correspond to the accepted (A), rejected (R), and difference ($A - fR$) spectra. Inspection shows that it is possible to find a value for 'f' that optimally reduces

the portion of the accepted line shape that extends to energies below the full-energy peak. This factor depends on energy and orientation of the source relative to the GRS axis for thin sources. The reason why this procedure works is that although the Compton cross section is monotonically decreasing with increasing gamma-ray energy, the integral of this cross section over all scattering angles such that the energy deposited in the ACS is larger than some threshold, is nearly constant between about 200 keV and 1.0 MeV. This threshold is set at about 35 keV in the LP GRS.

The capability of the GRS to resolve gamma-ray lines emitted by a thick source is given in Fig. 3 using a Pu–Be source immersed in a 30 cm diameter by 30 cm high container of wax. Inspection shows that the choice of $f = 4$ optimally removes the Compton continuum of both the 4.4 MeV (from $^{12}C^*$) and 2.2 MeV (from n(p,d)γ) lineshapes. We have verified (but do not show here) that this same factor achieves similar results for all thick gamma sources between 0.511 and 7.64 MeV. The choice of $f < 4$ yields an incomplete subtraction, which is nevertheless an improvement over the un-subtracted accepted spectra.

We do not presently have a quantitative explanation for this result but believe that it stems from two

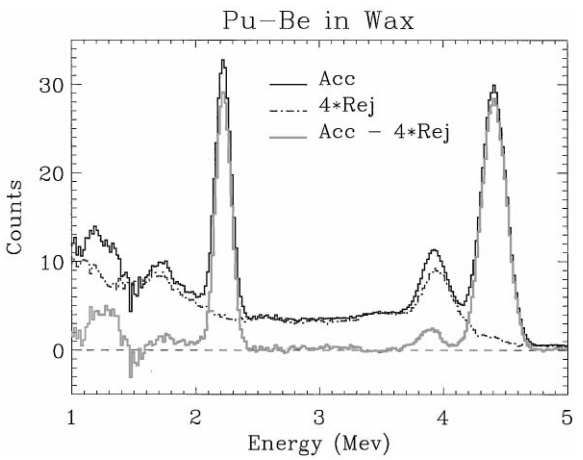

Fig. 3. Pulse height spectra of accepted (A), rejected (R), and ($A - 4R$) measured by the GRS using a wax-moderated Pu–Be source that illustrate its ability to remove the Compton continuum of a thick source.

separate functions served by the ACS; (1) rejection of events that Compton scatter from the BGO to the ACS, and (2) rejection of those events that scatter from the ACS to the BGO. Whereas the latter inscatter events cancel similar interactions that occur within the thick source, they do not exist (and hence rejected spectra remain unbalanced) in the thin sources. In consequence, the values of f needed to remove the Compton continuum in thin low-energy gamma-ray sources (such as the ^{137}Cs spectra shown in Fig. 2) are smaller (the Compton cross section increases with decreasing gamma-ray energy) than those needed for high-energy sources. The procedure of using a constant value of f should therefore apply to lunar gamma-ray spectra because the Moon is by nature, a thick source of gamma rays.

Fast neutrons having energies between about 0.5 and 8.0 MeV are measured using the ACS of the GRS. This task is achieved by filtering all detected events to isolate those characterized by a double interaction (the category-3 and -4 events) that are correlated in time through an exponentiation time constant of about 2.2 μs. The first interaction of this pulse-pair event corresponds to multiple (n,p) collisions in the plastic that moderate the incoming fast neutrons to thermal and epithermal energies. The second interaction corresponds to the $^{10}B(n,\alpha)^7Li^*$ reaction. Identification using both the measured time between consecutive interactions and the energy deposited in the scintillator in the second interaction (which corresponds to the Q-value of the reaction), then signals a fast neutron that has lost all of its incident energy in the scintillator. The pulse height of the first pulse of the pair then provides a measure of the energy of the incident fast neutron. This type of detector was successfully demonstrated in low-Earth orbit [1]. A side benefit of the LP GRS design is that it can be used to provide a very sensitive measure of thermal and epithermal neutrons through identification of coincident plastic and BGO events having pulse heights consistent with the charged-particle recoil component of the $^{10}B(n,\alpha)^7Li^*$ reaction in the ACS and the 478 keV gamma ray from decay of the first excited state of $^7Li^*$ in the BGO. This task is implemented using a field-programmable gate array (FPGA) in the GRS front-end electronics.

3. The neutron spectrometer (NS)

The neutron spectrometer (NS) consists of a matched pair of ^{3}He gas proportional counters. They have active volumes that are 5.7 cm in diameter and 20 cm in length, and are pressurized to 10 atm. One of the counters is covered by a 0.63 mm thick sheet of Cd and so responds only to epithermal neutrons, while the other is covered by a 0.63 mm thick sheet of Sn, and so responds to both thermal and epithermal neutrons. The difference in their counting rates yields a measure of the thermal neutron flux. These rates are controlled by window discriminators that cover the 763 keV peaks in measured pulse-height spectra, using an FPGA in the NS front-end electronics.

4. Operation of the GRS and NS in lunar orbit

Lunar Prospector was launched on 6 January 1998 and achieved its final mapping orbit on 16 January. This orbit is polar and circular at an altitude between 80 and 120 km. Sample spectra from the GRS and NS that illustrate the excellent quality of the data are shown in Fig. 4. Accepted and rejected gamma-ray spectra summed over about 12 h (6 lunar orbits) are shown in the top two panels in the right-hand column. Construction of $(A - 3R)$ shown at the right achieves optimal subtraction of the gamma-ray continuum above about 8 MeV. We note that although the choice of $f = 3$ is not optimal for full subtraction of the Compton continuum (as shown in Fig. 3), the resultant lunar gamma-ray spectrum at high energies reveals a relatively clean definition of several full-energy peaks. The 478 keV peak in the BGO and the charged-particle recoil peak in the ACS are shown in the next lower pair of panels (category-2 events). They are generated by thermal and epithermal neutrons in the GRS. They provide both a measure of the intensity of these neutrons and a robust and continuous gain calibration for the GRS. The top pair of panels in the left-hand column demonstrate the very clean identification of fast neutrons. The $\exp(-t/\tau)$ time correlation coming from the ^{10}B(n,α)^{7}Li* reaction at early times (after subtraction of $B\exp(-R_0 t)$ that result from chance coincidences at late times) is seen to be quite clean at the left. The ACS spectrum of second pulses at the right also shows a very clean spectrum of charged-particle recoils, accompanied some of the time by the Compton interaction of a 478 keV gamma ray. Finally, the pulse-height spectra of Sn and Cd covered ^{3}He gas-proportional counters are shown at the left and right in the bottom two panels in the left-hand column, respectively. The dashed lines in both spectra were measured during a 12 h period when Lunar Prospector was in transit between Earth and Moon. Inspection shows these backgrounds to be negligible for measurements made in lunar orbit (where they should be reduced by about

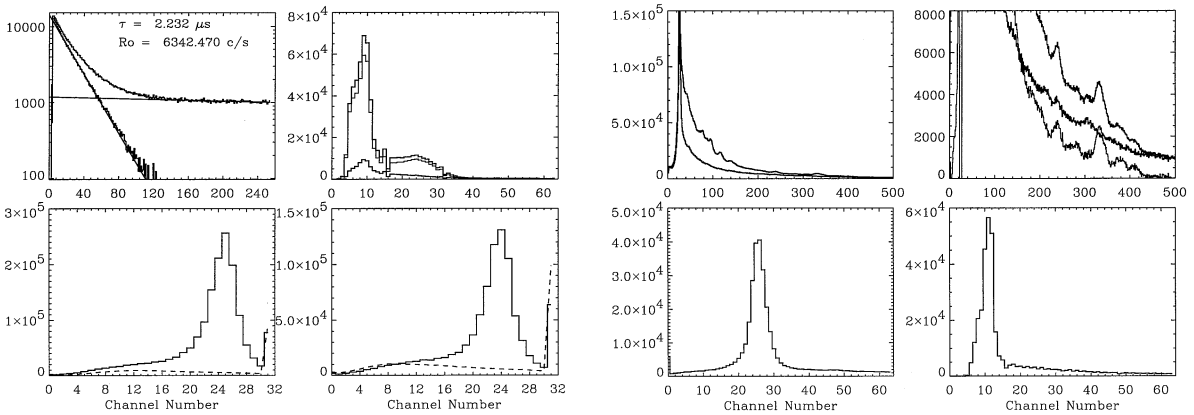

Fig. 4. Pulse height spectra measured during the first 12 h of 10 April, 1998 by the GRS and NS in lunar mapping orbit that illustrates the quality of data. See the text for details.

a factor of two because the Moon blocks out nearly half the sky).

In summary, Fig. 4 shows that the data quality of both the GRS and NS in lunar orbit are excellent. We therefore expect to attain all the scientific objectives listed in Section 1.

Acknowledgements

The success of all three Lunar Prospector Spectrometers is owed to the intense effort expended by many individuals. Most prominent are R. Black, T. Chinn, D. Everett, K. Henneke, J. Kolar, G. Longmire, T. Polette, J. Shirley, S. Storms, and G. Thornton. This work was supported in part by NASA and conducted under the auspices of the U.S. Department of Energy.

References

[1] W.C. Feldman, G.F. Auchampaugh, R.C. Byrd, Nucl. Instr. and Meth. A 306 (1991) 350.
[2] C.L. Melcher et al., IEEE Trans. Nucl. Sci. NS-32 (1985) 529.